DOI: 10.1002/chem.200701587

High-Relaxivity Magnetic Resonance Imaging (MRI) Contrast Agent Based on Supramolecular Assembly between a Gadolinium Chelate, a Modified Dextran, and Poly-β-Cyclodextrin

Elisa Battistini,[a] Eliana Gianolio,[b] Ruxandra Gref,[c] Patrick Couvreur,[c] Silvia Fuzerova,[b] Mohammad Othman,[c] Silvio Aime,[b] Bernard Badet,[a] and Philippe Durand*[a]

Abstract: Nanosized contrast agents have great potential in magnetic resonance molecular imaging applications for clinical diagnosis. This study proposes new nanoparticles spontaneously formed under mild conditions and composed of a noncovalent adduct between a gadolinium complex, a polymer of β-cyclodextrin (pβCD: MW $1.5\times10^6\,g\,mol^{-1}$) and a dextran grafted with alkyl chains (MD). The formation of this supramolecular nanoassembly is based upon a "lock-and-key" recognition process in which the hydrophobic alkyl chains of MD and the adamantyl moieties of macrocyclic Gd^{III} chelates are included in the cavities of pβCD. The large number of βCDs contained in the pβCD resulted in the formation of 200 nm diameter nanoparticles, each entrapping 1.8×10^5 molecules of a low-molecular-weight Gd complex. This system, which exhibits a great relaxivity enhancement ($48.4\,mM^{-1}s^{-1}$, at 20 MHz and 37 °C) compared to the Gd^{III} chelate itself ($5.2\,mM^{-1}s^{-1}$), appears to be a promising strategy for the in vivo targeted delivery of Gd^{III} complexes. The mechanisms of particle formation, conjugation strategies, and relaxometric characterizations in the field of contrast-enhanced magnetic resonance imaging are discussed.

Keywords: contrast agents · cyclodextrins · gadolinium · MRI (magnetic resonance imaging) · nanoparticles · noncovalent interactions

Introduction

Magnetic resonance imaging (MRI) is a powerful, noninvasive diagnostic technique with high spatial resolution. In an MR image, the contrast is the result of a complex interplay between instrument parameters and intrinsic differences in the relaxation rates of tissue water protons. In many cases the contrast can be improved by using a contrast agent (CA), such as a Gd^{III} chelate, which locally reduces the proton relaxation times. The magnitude of this effect on the longitudinal relaxation time T_1 (or transverse relaxation time T_2) is measured as relaxivity r_1 (or r_2, respectively) normalized to 1 mM concentration at a given magnetic field strength and is used to evaluate the efficacy of the agents.[1–4] Most of the currently used extracellular agents are nonspecific and far less efficient than predicted by theory.[2] This means that in order to achieve enough contrast in an MR image, concentrations of CA higher than 50 μM have to be reached in a localized area.[5,6] A very active search is under way for targeting contrast agents,[5,7–10] that is, for systems able to delineate lesions by the specific design of molecules for a given pathology. As the concentration of the targets may be very low (typically 10^{-9}–$10^{-13}\,mol\,g^{-1}$ of tissue), it is necessary to reach high concentrations of Gd^{III} chelate with high relaxivity at the site of interest.[11] This goal may be pursued by 1) using polymers containing covalently bound CA units (dendrimers,[12] polymers and polysaccharides,[13–17] poly amino acids and proteins);[18,19] 2) exploiting self-assembly[20–29] or noncovalent

[a] Dr. E. Battistini, Dr. B. Badet, Dr. P. Durand
CNRS, UPR 2301
Institut de Chimie des Substances Naturelles (ICSN)
1 Avenue de la terrasse, 91198 Gif-sur-Yvette (France)
Fax: (+33) 169-077-247
E-mail: philippe.durand@icsn.cnrs-gif.fr

[b] Dr. E. Gianolio, S. Fuzerova, Prof. S. Aime
Department of Chemistry I.F.M., University of Torino
Via P. Giuria 7, Torino 10125 (Italy)

[c] R. Gref, P. Couvreur, M. Othman
UMR CNRS 8612, Faculty of Pharmacy, Paris-Sud University
5 rue Jean Baptiste Clément, 92290 Châtenay-Malabry (France)

Supporting information for this article (equations used for the PRE method and the analysis of the ^{17}O NMR and NMRD data, the ^{13}C NMR spectra of compounds and HPLC analyses) is available on the WWW under http://www.chemeurj.org/ or from the author.

interactions between a suitably functionalized chelate and a macromolecular substrate;[6,30–32] and 3) using nanoscale cargoes such as liposomes and nanoparticles.[5,8,33–37] From these routes, the nanocarriers have recently shown a significant degree of success in providing positive contrast agents with remarkable gadolinium payload that can also be functionalized for molecular targeting. Many of these Gd^{III}-containing assemblies behave as colloidal carriers which, in addition to the increased relaxivities, have valuable pharmacological characteristics.[38] Nanoparticles therefore appear as promising candidates for molecular imaging, and there is a growing need for more powerful new systems. In the pursuit of different in vivo delivery methods, one can change the size, charge, and surface properties of these carriers, as well as the Gd^{III}-loading mode, by adding new ingredients to the mixture or by variation of preparation methods. In this context the host–guest type interactions with cyclodextrin (CD) have been exploited to obtain large supramolecular structures[39,40] and especially high-molecular-weight adducts of poly-β-cyclodextrin (pβCD) (average MW of 6–130 KDa) with suitably functionalized chelates, leading to an efficient relaxation enhancement.[32,41–45] However, all the previously described systems using CD have been limited to a moderate β-cyclodextrin (βCD) content and a consequent low amount of loaded Gd^{III}.

Recently, a new stable supramolecular nanoassembly based on noncovalent host–guest interactions exhibiting high βCD content has been described.[46] The polymers involved in the formation of these nanoparticles are a dextran functionalized with alkyl chains (MD) and a high molecular weight pβCD. The matching of these stable structures gives a supramolecular adduct of about 200 nm diameter that results from the formation of inclusion complexes between hydrophobic alkyl chains grafted on the polysaccharide (dextran) and the βCD cavities of the polymer. Several specificities make this nanosystem a promising candidate for the encapsulation of Gd^{III} derivatives: 1) it is prepared in a convenient one-step procedure, without the use of organic solvents and surfactants, exploiting a simple and biocompatible technology and meeting in this way the requirements of public health agencies;[46] 2) it constitutes a potential carrier of very high Gd^{III} payload, since about half of the numerous βCD cavities remain free to entrap a lipophilic Gd^{III} chelate through host–guest-type interactions;[46] and 3) the high number of water molecules contained in the nanoparticles (70 wt% of the nanogel is water)[47] would result in a remarkable proton density surrounding the Gd^{III} necessary for high relaxivity.

In this paper we describe the formation and the relaxometric properties of highly loaded Gd^{III} nanoparticles through a three-component assembly based on noncovalent interactions (Figure 1). A new Gd^{III} chelate bearing an adamantyl moiety, which was designed to form a host–guest adduct with βCD and pβCD, has been synthesized, and its interaction has been quantified by using the proton relaxation enhancement (PRE) method. Different conditions have been tested in order to optimize the entrapment of the Gd^{III} chelate in the pβCD/MD nanoparticles while maintaining their size and stability. The effect of the complexation with pβCD or pβCD/MD on the proton relaxivity of the Gd^{III} chelate has been measured. To determine the influencing parameter, namely the water exchange rate and rotational correlation time, variable-temperature ^{17}O NMR and multiple-field ^{1}H NMRD (nuclear magnetic relaxation dispersion) studies have been performed.

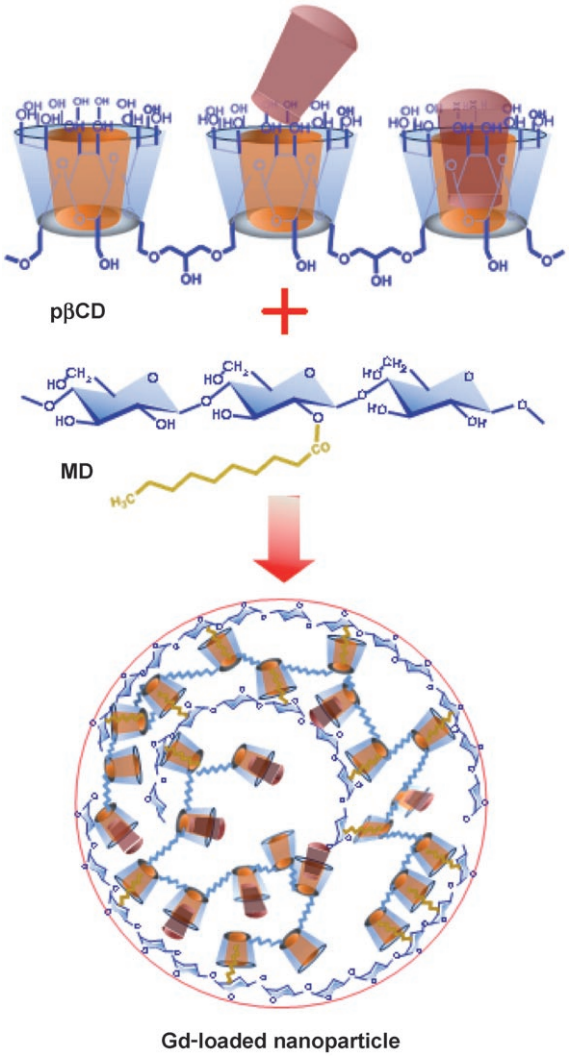

Figure 1. Formation of Gd^{III}-loaded nanoparticles through a supramolecular three-component assembly: Gd^{III} chelate/pβCD/MD. The alkyl chains functionalizing dextran are in yellow, the Gd^{III} chelate is in violet.

Results and Discussion

The Gd^{III} complex

Design and synthesis: A new contrast agent was designed to form a host–guest inclusion complex with βCD. It is based on the cyclic polyaminocarboxylate DO3A (DO3A = 1,4,7,10-tetraazacyclododecane-1,4,7-triacetic acid) template

linked through a spacer to a known guest ligand of cyclodextrin. The cyclic DO3A was chosen, rather than a linear analogue, because of its known thermodynamic and kinetic stability. Among the possible hydrophobic guests of βCD,[48,49] adamantyl appeared as the most appropriate, since it fits perfectly inside the βCD cavity, resulting in suitable association constants (10^3–10^5 M^{-1}).[50,51] Crystal structures of the complexes between adamantyl derivatives and βCD have confirmed the inclusion of this moiety inside the cavity.[52,53] Moreover the bulkiness of the adamantyl groups prevents the formation of large hydrophobic microdomains (as is the case with alkyl tails) and therefore avoids the self-association of the contrast agent.[54] DO3A and adamantane were connected through an acetamide spacer, although it is known that in some cases this function is deleterious for the water-exchange-rate parameter.[55,56] In fact, it represents a good compromise between the necessity of placing the adamantyl away from the bulky DO3A moiety to facilitate its optimum fitting in the βCD cavity and the need for overall rigidity of the entity in order to optimize the rotational correlation time of the contrast agent (τ_R). To our surprise only one linear polyaminocarboxylic Gd^{III} ligand bearing an adamantyl moiety has been reported.[57]

The synthesis of compounds **1**–**5** is shown in Scheme 1. The Gd complex **5** was obtained in a four-step process from triethyl ester **2** and 1-adamantanamine, which was first acylated with bromo acetylbromide by using a modified procedure.[58] The bromo acetamide derivative was then used to alkylate the macrocycle **2** in 97% yield. Steric congestion in the structure of **3** was evidenced by the broadening of resonance signatures (273–373 K) in both ^1H and ^{13}C NMR spectra resulting from slow conformational interconversion. Saponification of the tetra-alkylated cyclen **3** by a strong anion exchange resin avoids side formation of salts during this step. The complex was formed under pH-controlled conditions with a stoichiometric amount of $GdCl_3$ at room temperature. Finally, special attention was paid to the removal of salts through gel filtration chromatography to avoid any problem of instability of the nanosystem during the entrapment. The Gd complex **5** was therefore obtained in a four-step process and 15% overall yield.

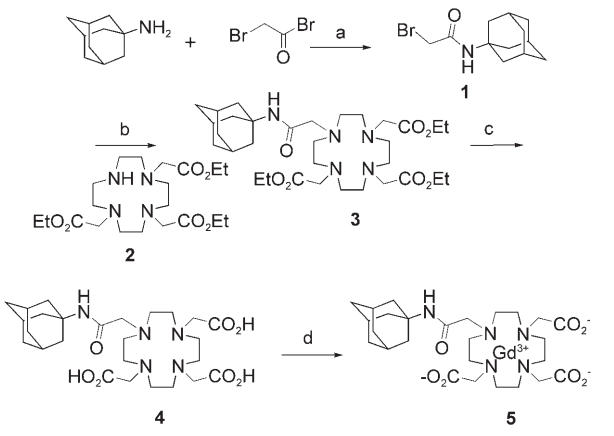

Scheme 1. Synthesis of the Gd^{III} chelate: a) CH_2Cl_2, Na_2CO_3, RT; b) CH_3CN, K_2CO_3, RT; c) $EtOH/H_2O$, AG1-X4 resin (OH Form), RT; d) $GdCl_3$, H_2O, RT.

Relaxivity: For the chelate **5**, the millimolar relaxivity r_1 of 5.2 $mM^{-1}s^{-1}$, measured at 20 MHz and 298 K, is in agreement with reported values for molecules with comparable molecular weight.[3] The pH dependence study of the relaxivity (data not shown) indicates that the Gd^{III} chelate is stable in the range of pH 4–12. At more acidic pH the protonation of the carboxylic groups of the complex makes it unstable, subsequently increasing the relaxivity.

The host–guest adducts with βCD and pβCD—relaxometric characterization of binding parameters: The increase of the relaxivity of a Gd^{III} chelate caused by the lengthening of its reorientational correlation time τ_R is a well-known phenomenon. Usually, the increase of τ_R results from the formation of adducts between the paramagnetic chelate and a slowly tumbling substrate. In the context of this work, one could expect that the non-covalent interaction of **5** with the cyclodextrin hosts will result in an increase of relaxivity, as previously described for related systems.[32,44] The relaxometric characterization of the adducts with both the monomer βCD and the high-molecular-weight pβCD was performed. Binding parameters (the affinity constant K_A, the number of equivalent and independent binding sites n and the relaxivity of the supramolecular adduct r_1^b) were determined using the proton relaxation enhancement (PRE) method, which considers the relaxation enhancement derived from the formation of the adduct.[19] The method involves measuring the water proton relaxation rate in the presence of the complex and increasing amounts of βCD or pβCD (Figures 2 and 3, respectively).

Considering the equilibrium, **5** + H ⇄ **5**/H, in which H is the host (βCD or pβCD) and **5**/H is the host–guest adduct, the affinity constant K_A is given by Equation (1), in which [nH]

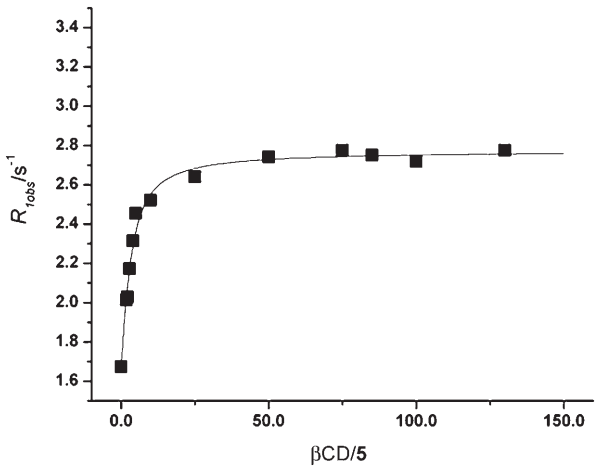

Figure 2. Water proton relaxation rate of an aqueous solution of 0.1 mM **5** upon addition of increasing amounts of βCD. The solid line is the result of the fitting to Equation (2) using parameters reported in Table 1.

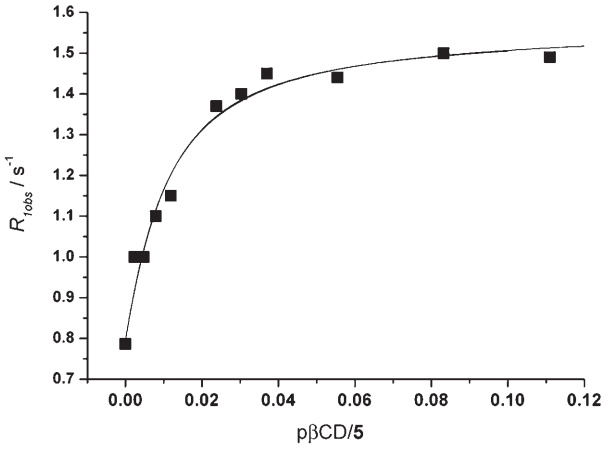

Figure 3. Water proton relaxation rate of an aqueous solution of 0.1 mM **5** upon addition of increasing amounts of pβCD. The solid line is the result of the fitting to Equation (2) using the parameters reported in Table 1.

indicates the concentration of the equivalent and independent binding sites.

$$K_A = \frac{[\mathbf{5}/\mathrm{H}]}{[\mathbf{5}][n\mathrm{H}]} \quad (1)$$

In the aqueous solution containing the two interacting species, the measured longitudinal proton relaxation rate, R_{1obs}, is given by the sum of the contributions arising from the unbound and the bound species as well as from the diamagnetic contribution of the host, R_{1H}, as given by Equation (2), in which r_1 and r_1^b are the millimolar relaxivities of the unbound and bound **5** chelate, respectively.

$$R_{obs} = (r_1[\mathbf{5}] + r_1^b[\mathbf{5}/\mathrm{H}])1000 + R_{1H} \quad (2)$$

Combination of Equations (1) and (2) allows correlation of the measured R_{1obs} to the binding parameter K_A and n (see equations of the PRE method in the Supporting Information). For the determination of K_A for the βCD, a fixed concentration of Gd^{III} chelate was titrated with βCD (Figure 2). By fitting the curve obtained to Equation (2), a K_A value of $4.9\times10^3\,M^{-1}$ and r_1^bc value of $9.6\,mM^{-1}s^{-1}$ were calculated (Table 1).

Table 1. Binding parameters relative to the supramolecular adducts of **5** with βCD and pβCD.

Host	K_A[a] [$10^3\,M^{-1}$]	n[b]	r_1^b[a,c] [$mM^{-1}s^{-1}$]	r_1^b/r_1[d]
βCD	4.9±0.54	1	9.6±0.08	1.8
pβCD	6.3±1.10	185	14.8±0.40	2.8

[a] Determined from the fitting of the titration curves (Figures 2 and 3), see Supporting Information for equations. [b] See text for the determination of n in the case of pβCD. [c] r_1^b is the relaxivity of bound **5**. [d] Relaxivity enhancement, r_1 relaxivity of **5** ($5.2\,mM^{-1}s^{-1}$).

To determine the parameters K_A and n for the pβCD, two different kinds of titrations were performed. In the first, the titration of a fixed concentration of Gd complex **5** with pβCD resulted in an increase of the relaxation rate (Figure 3). The fitting of the obtained curve to Equation (2) gave $K_A = 6.3\times10^3\,M^{-1}$ and $r_1^b = 14.8\,mM^{-1}s^{-1}$ (Table 1). In the second, a fixed concentration of the pβCD was titrated with **5** (Figure 4). The water proton relaxation rate increased linearly with the concentration of the added **5** until a slope breaking point, corresponding to the saturation of the polymer and to the contribution of additional free Gd^{III} chelate remaining in solution, was observed. The **5**/pβCD ratio of approximately 185 found at this point corresponds roughly to n.[19] This Gd^{III} payload was not reachable with previously reported pβCD.

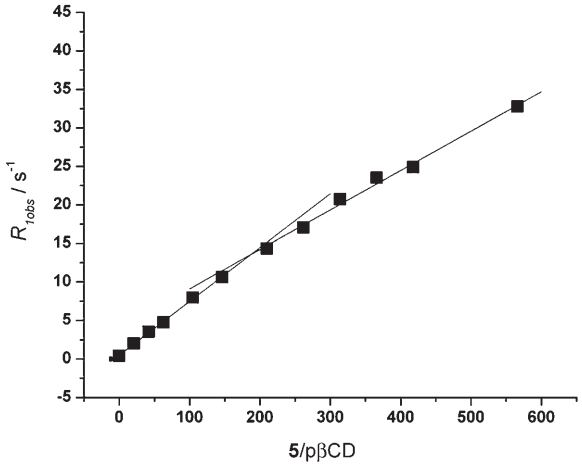

Figure 4. Water proton relaxation rate of an aqueous solution of 5 μM of pβCD upon addition of increasing amounts of **5**.

The measured association constants for the adduct of **5** with the different forms of βCD (Table 1) are higher than values reported for most other adducts of monofunctionalized Gd^{III} chelates with βCD.[59–61] The relaxivity enhancements observed upon formation of the supramolecular adducts with βCD and with pβCD (Table 1) are similar to values reported for related systems.[32,41,44,60,62–64] The rather limited enhancement obtained with pβCD, in spite of its high molecular weight (10^3–2.6×10^3 KDa), is classical for this linear polymer and has been assigned to the predominance of the segmental motions over the rotational correlation time, which becomes independent of molecular weight above 10 KDa.[65] Nevertheless, these results demonstrate that adamantane-functionalized **5** forms inclusion complexes with βCD and its polymeric form; this was a prerequisite for the following study on the engineered supramolecular nanoassemblies.

Nanoparticles containing the Gd^{III} chelate

Preparation: The MD-pβCD nanoparticles were prepared by simply mixing two aqueous solutions containing the two respective polymers involved. It was previously established

that practically all the alkyl chains of MD were included within the cyclodextrin cavities of pβCD, leaving about half still available for the complexation of the molecules of interest.[46] Nanoparticles containing Gd^{III} were obtained in a similar way, by mixing at room temperature equal volumes of two aqueous solutions containing a preformed pβCD/**5** host–guest adduct and MD, respectively (Figure 1). To demonstrate the formation of the three-component nano-assembly, several studies were carried out. First, the influence of the concentration of the nanoparticle components on the size stability of the particles and on the entrapment of the Gd^{III} chelate was evaluated. Different nanoparticle preparations corresponding to different concentrations of the three components, pβCD/**5**/MD, were prepared as described above. A first assay with respective concentrations of 5/0.5/5 mg mL^{-1} led to precipitation, indicating formation of aggregates and instability of the nanoparticles. This phenomenon was found to be independent of the presence of Gd^{III} chelate, since the mixing of the two components pβCD and MD in the same concentration range led to the same result. For this reason the study was performed at lower concentrations of the two polymers. Three preparations (Table 2) were investigated in detail. The size of the nanoparticles in solution and their homogeneity (polydispersity) were determined by quasi-elastic light scattering (QELS) at two different time points after their preparation. The amount of entrapped **5** was determined as the difference between the total amount added and the amount of free Gd^{III} chelate. The latter was obtained by quantification of **5** in the supernatant after ultracentrifugation of the nanoparticle preparation using Evans' method.[66] We noticed a small effect of the concentration of **5** on the size of the nanoparticles (compare B/C, Table 2) due probably to entrapment of the chelate, and almost no effect of the concentration of the polymers (compare A/B, Table 2). For all the preparations the polydispersity was lower than 0.2, showing a monomodal population with narrow size distribution. Moreover, the size and the polydispersity were constant over 36 h, demonstrating the stability of the Gd^{III}-loaded supramolecular system.

Table 2. Effect of the components ratio on the size, stability, and **5** entrapment for the nanoparticles.

Preparation[a]	Component ratio[b]	$d^{30\,min}$ [c] (±SD) [nm]	$d^{36\,h}$ [d] (±SD) [nm]	PI[e]	E_{Gd}[f] (±SD) [%]
A	2.5/0.5/2.5	214 (±2.6)	211 (±1.6)	<0.2	41 (±2.9)
B	1.25/0.5/1.25	200 (±2.8)	190 (±1.9)	<0.2	24 (±1.7)
C	1.25/0.25/1.25	132 (±1.6)	130 (±0.97)	<0.2	16 (±1.7)

[a] See Experimental Section. [b] Concentrations in the preparation for the three components βCD/**5**/MD respectively expressed in mg mL^{-1}. [c] Mean hydrodynamic diameter of nanoparticles from QELS determined 30 min after their preparation. Each measurement was repeated three times for two minutes at room temperature at an angle of 90°. SD = standard deviation. [d] As [c] but determined 36 h after their preparation. [e] PI: polydispersity index. [f] Percentage of **5** entrapped in the nanoparticle on total **5**. Determined 30 min after their preparation as described in the text.

Among the three concentration ratios tested the highest percentage of **5** entrapped was obtained for preparation A (Table 2). The previously mentioned instability of the nanoparticles formed from more concentrated solutions of polymers (see above) prevented the increase of the pβCD/MD concentrations tested. The gain in percentage of entrapment observed for preparation A in comparison to preparation B can be assigned to the higher concentration of nanoparticles formed rather than to a higher amount of Gd^{III} entrapped in each of them. Indeed, the ratio of this percentage (E_{Gd}, Table 2) on the total concentration of polymers (5 mg mL^{-1} for A and 2.5 mg mL^{-1} for B) is slightly lower for preparation A (8.2 versus 9.6). In the case of preparation C, this ratio is lower (6.4), indicating a less efficient entrapment. In this context, preparation A was considered as the best compromise for the studied parameters and was chosen for further investigation. No variation of the percentage of entrapment was observed over a period of 36 h, confirming the stability of the host–guest adduct in the nanoparticles.

To evaluate the maximum amount of **5** that can be internalized without destabilizing these nanoparticles, preparations with a concentration ratio of 2.5/*x*/2.5 were used. The concentration of the **5** (x) was varied from 0.5 to 3 mg mL^{-1} (Table 3). The payload of Gd^{III} chelate (P_{Gd}) for each mixture was determined by using Equations (3) to (6), in which V_{NP} and d are the volume and the mean hydrodynamic diameter of a particle, respectively, and N_{NP} is the number of nanoparticles in 1 mL of preparation. These equations are based upon the measurement of the amount of gadolinium entrapped and on the particle size.[37]

Table 3. Effect of the **5** concentration on the size, stability, and **5** entrapment.

x[a] [mg mL^{-1}]	$d^{30\,min}$[b] (±SD) [nm]	$d^{3\,h}$ [c] (±SD) [nm]	PI[d]	Gd_b[e] [10^{-9} M]	P[f]
0.5	214 (±2.6)	215 (±1.6)	<0.2	304	1.8×10^5
2.0	418 (±143)	940 (br)	>0.5	800	3.7×10^6
3.0	466 (br)	1480 (br)	>0.5	1360	8.3×10^7

[a] x is the concentration of **5** in preparations containing 2.5 mg mL^{-1} of each polymer pβCD/MD. [b] See footnote [c] in Table 2. [c] Mean hydrodynamic diameter of nanoparticles from QELS determined 3 h after their preparation, SD = standard deviation, br = broad. [d] PI: polydispersity index. [e] Amount of entrapped **5** determined as described in the text. [f] P: Payload or unit of **5** entrapped per nanoparticle, determined as mentioned in the text.

$$V_{NP} = \frac{1}{6}\pi d^3 \quad (3)$$

$$N_{NP} = W_{NP}/(d_{NP}\, V_{NP}) \quad (4)$$

$$U_{Gdb} = Gd_b N \quad (5)$$

$$P_{Gd} = U_{Gdb}/N_{NP} \quad (6)$$

The weight of nanoparticles formed in 1 mL of preparation, W_{NP}, is assumed to be the sum of the weight of the

polymers pβCD and MD used. The value of the density of the nanoparticle, d_{NP}, is assumed to be 1. The parameter U_{Gdb} is the number of **5** entrapped in the nanoparticles formed from 1 mL of preparation, Gd_b is the mole number of **5** entrapped, and N is Avogadro's number. The size, polydispersity, and amount of Gd^{III} chelate entrapped for the different mixtures were determined as described for the previous study. The noticeable increase of the payload at the highest ratios of **5** (from 1.8×10^5 to 8.3×10^7 **5**/NP), was associated with an increase in the size of the nanoparticles (Table 3). Diameters above 400 nm were obtained for concentrations of **5** higher than 2 mg mL^{-1}; polydispersity above 0.5 indicated the coexistence of several nanoparticle populations. This destabilization might result from competition for the β-cyclodextrin cavity between the adamantyl moiety and the lauryl chains anchored to the modified dextran.[39]

From this series of experiments it appears that with regard to the size, the stability, and the capacity for Gd^{III} entrapment, the optimized conditions were obtained for preparation A. The measured diameter of around 200 nm and the stability over 36 h are compatible with intravenous administration.[67] The high value of almost 1.8×10^5 units of Gd^{III} chelate entrapped per particle is definitely a very promising result in the context of MRI. Indeed, the best reported results in the literature were about 9×10^4 units of Gd^{III} per fluorocarbon nanoparticle of about 250 nm diameter,[68] and only about 4×10^4 Gd^{III} per liposome of 100 nm diameter.[69]

Relaxometric characterization: The main objective of this study was to obtain a supramolecular system with a good Gd^{III} payload and a high relaxivity. Having achieved the first requirement, we needed to study the relaxometric behavior of the nanoparticles and to compare it with the free Gd^{III} chelate and its host–guest adducts with βCD and pβCD. The residence lifetime of the water molecule coordinated to the metal center (τ_M) is one of the key parameters responsible for the relaxivity of chelates immobilized on slowly moving substrates. The τ_M of **5** was determined from the study of the temperature dependence of the transverse relaxation rate (R_{2p}^O) for the ^{17}O water nuclei (Supporting Information, Figure 2). The R_{2p}^O values increase with the temperature until τ_M becomes short enough with respect to R_{2M}^O (transverse relaxation rate of the metal-bound ^{17}O water nucleus), and this causes a decrease in R_{2p}^O with a further increase in temperature. The resulting bell-shaped curve was fitted to equations first proposed by Swift and Connick[70,71] (all relevant equations and the other fitting parameters are given in the Supporting Information) to give the τ_M value of 513 ± 73 ns at 298 K. This value, which is almost twice that determined for [Gd(DOTA)][2,72] (244 ns) might be explained by considering the structure of the complex. A reasonable assumption is that the presence of the amido group in the spacer slows down the exchange rate of the coordinated water molecule, as already observed upon carboxylic acid replacement by this function.[73,74] Unfortunately, the high concentration of Gd^{III} chelate required for the ^{17}O NMR experiment is incompatible with that of nanoparticle preparation A, and the residence lifetime of the water molecule coordinated to the metal in the supramolecular construct could not be determined by this method. For the rest of the study it was assumed to be identical to the value found for the free Gd^{III} chelate.

The measurement of water proton relaxation rate over an extended range of magnetic field strengths (0.01–80 MHz; the NMRD experiment) is a complementary method for the complete characterization of a paramagnetic complex.[70,72] The resulting plot of r_1 versus the proton Larmor frequency, the NMRD profile, for **5** is reported in Figure 5. All the

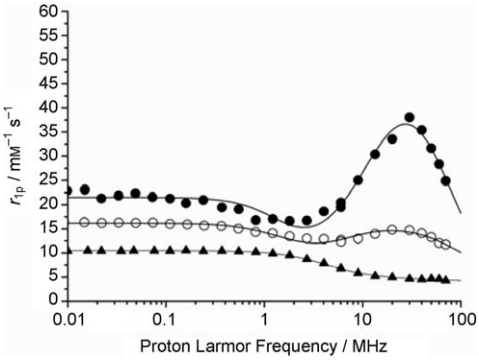

Figure 5. Overlapping of $1/T_1$ NMRD profiles at 298 K and neutral pH of 0.3 mM solution of **5** (▲), the adduct with pβCD (○), and with pβCD/MD (●).

data were analyzed by using the classical inner sphere[75,76] and outer sphere theories.[77] The inner and outer sphere contributions are determined by several structural and dynamic parameters (Δ^2, τ_V, τ_M, τ_R, q, r, a, D). The possibility of fixing the values of some of the parameters involved makes the determination of others more accurate. The analysis of the NMRD profiles collected in recent years for a series of structurally similar Gd^{III} chelates provided us with reliable estimates for some relaxation parameters. In particular, the value of "q" (number of coordinated water molecules) was assumed to be 1, as expected for all DOTA derivatives; the distance "r" between the Gd^{III} ion and the protons of the coordinated water molecule was fixed at 3.1 Å, and the distance "a" between the Gd^{III} ion and the outer sphere water proton nuclei was set at 3.8 Å; the solute–solvent diffusion coefficient (D) was fixed at 2.24×10^{-5} cm^2 s^{-1}. The exchange lifetime (τ_M^{298}) was fixed to the value previously obtained for **5** from ^{17}O-NMR studies (513 ns). The shape of the profile shows dispersion between 3 and 8 MHz, and two plateaus in the regions of low and high magnetic field. The τ_R value (81 ps) calculated from the best fitting of the data is in the range usually found for molecules with a similar molecular weight (for Δ^2, τ_V parameters see Supporting Information).[78]

To assess the efficacy of the nanoparticles (preparation A) and to evaluate the parameters governing their relaxivity, the NMRD profile between 0.01 and 80 MHz was recorded

at 25 °C (Figure 5). The profile shows that this system possesses high relaxivity values at all fields, with a marked peak centered at 30 MHz. The values are similar to those reported for other Gd^{III} chelates bound to a macromolecule, with a peak at around 30 MHz caused by an increase in the reorientational correlation time (τ_R).[2] Experimental data were first analyzed by using the Solomon–Blombergen–Morgan inner/outer-sphere model,[75,76]considering one water molecule in the inner coordination sphere of the Gd^{III} chelate ($q=1$) and fixing the exchange lifetime (τ_M) to the value obtained from ^{17}O NMR studies for **5**. The other structural and dynamic parameters (r, a, D) were fixed to the values previously used for the free ligand (see above). Actually, this quantitative analysis of the NMRD profile based on the simple inner/outer-sphere model was not entirely satisfactory. To obtain a better fitting, the observed relaxivities were assumed to also receive contributions from protons of one water molecule present in the second coordination sphere of the Gd^{III} chelate at a distance of approximately 4 Å. The second-sphere water molecule was defined as the water molecule held in the second coordination shell of Gd^{III} through hydrogen bonding with the polar groups present in the ligand.[79] This second-sphere contribution was analyzed on the basis of the Solomon–Blombergen–Morgan model suitably modified by introducing a generic correlation time (τ_{ss}), which deals with the modulation of the dipolar interaction of the second-coordination-sphere water molecules (exchange and/or rotation). For the nanoassembled nanoparticles at 25 °C, a τ_R value of 3.5 ns and a τ_{ss} value of 2.95 ns were calculated from the best fitting procedure of the data. Surprisingly, the τ_{ss} value appears to be very similar to the τ_R determined for the overall supramolecular assembly. Although we are conscious that this result is still an approximation, highly dependent on the model used for the fitting, it suggests that the motion of this second-sphere water molecule may be considered interdependent with that of the Gd^{III} chelate. It is probably held in the proximity of the paramagnetic metal through hydrogen bonding with some of the numerous hydroxyl groups provided by both the pβCD and MD polymers.

Moreover, since **5** is endowed with a rather long exchange lifetime of the coordinated water molecule, the relaxivity may be increased at physiological temperature (37 °C) compared with at 25 °C due to the increase of the water exchange rate. The increase of temperature induces an enhancement of the relaxivity at 20 MHz from 33.5 to 48.4 $mM^{-1}s^{-1}$. This increase in relaxivity could be ascribed neither to a partial release of free Gd^{III} nor to a size increase of the particles. Indeed, we have verified, using the methods previously described, that the size of the nanoparticles and the amount of Gd^{III} entrapped did not change between these two temperatures. These data simply outline the observation that the relaxivity is quenched by a long exchange lifetime at 25 °C, but this limiting factor may be reduced at 37 °C, at which the water exchange rate is faster ($\tau_M^{310}=315$ ns). The use of a Gd^{III} chelate endowed with a shorter exchange lifetime than **5** could bypass this quenching effect. The higher millimolar relaxivity of 48.4 $mM^{-1}s^{-1}$ found at physiological temperature compares very well with the value reported for other nanosystems.[33]

The comparisons of the NMRD profiles of the loaded nanoparticles with those of **5** and the pβCD/**5** adduct acquired under the same conditions definitely demonstrate their higher efficacy. Regarding the millimolar relaxivitiy at 298 K and 20 MHz, a sharp enhancement is observed from 5.2 $mM^{-1}s^{-1}$ for **5** to 14.8 and 33.5 $mM^{-1}s^{-1}$ once the adducts are formed with pβCD and pβCD/MD, respectively. Different fitting models have been used in the case of pβCD/**5** and loaded nanoparticles, because of a big difference in the fitting quality by using one model instead of the other. This has to be taken into consideration for the following comparisons. The high-field relaxivity peak associated with the molecular correlation time τ_R centered at 30 MHz is much higher for the nanoparticles than for the metal complex and even than for the host–guest adduct with pβCD (Table 4 and Figure 5). In this last case the best fitting of the NMRD profile was obtained by using the Solomon–Blombergen–Morgan model suitably modified according to the Lipari–Szabo approach (see Supporting Information) in which a shorter local and a longer global reorientational correlation time have to be accounted for. In fact, it is reasonable to think that in the pβCD adduct the Gd complex may be free to move independently of the supramolecular backbone constituted by the cyclodextrin linear polymer.

Table 4. Reorientational correlation times for the different forms of **5**.[a]

	τ_R [ps][b]			q_{ss}[c]	τ_{ss} [ps][d]
	τ_l	τ_g	S		
5/pβCD/MD		3527		1	2950
5/pβCD	220	2061	0.49	0	–
5		81		0	–

[a] The reorientational correlation times for the different forms of **5** were calculated from the fitting of NMRD profiles measured at pH 7.4 and 25 °C reported in Figure 5. During the fitting procedure some parameters were fixed; namely: the number of coordinated water molecules: $q=1$; the distance between Gd^{III} ion and the protons of the coordinated water molecule: $r=3.1$ Å; the distance of maximum approach of the outer sphere water proton nuclei: $a=3.8$ Å; the solute-solvent diffusion coefficient: $D=2.24\times10^{-5}$ cm^2s^{-1}; the exchange lifetime was fixed to the value previously obtained for **5** from ^{17}O-NMR studies: $\tau_M^{298}=513$ ns. [b] τ_l is the correlation time for the local motion, τ_g is the correlation time for global motion, S is the generalized order parameter, see Supporting Information. [c] Number of second-sphere water molecules. [d] See the text and Supporting Information.

On the other hand, in the case of the nanoparticle assembly, besides the contribution from one tightly bound second-sphere water molecule, the relaxivity enhancement clearly has to be attributed to the lengthening of the effective molecular reorientational motion ($\tau_R=3.5$ ns) of the Gd^{III} complex firmly entrapped in the supramolecular system without any chance of independent motions.

Conclusion

The present study describes a new paramagnetic contrast agent with high Gd^{III} payload and high relaxivity. The supramolecular assembly, resulting from the self-association of a hydrophobic modified dextran, a βCD polymer, and a functionalized Gd^{III} chelate, leads to homogeneous stable nanoparticles with diameter of about 200 nm, a payload of 1.8×10^5 units of Gd^{III} and a relaxivity r_1 of 48.4 $mM^{-1}s^{-1}$ at 20 MHz and 37 °C. This macromolecular Gd-based system is expected to be less toxic than that in which Gd^{III} chelate is covalently bound to a polymeric matrix, since it would follow the elimination pathway of the free low molecular weight complex. The MD/pβCD nanoparticles appear to be a good candidate for the delivery of contrast agents that could be further improved in terms of relaxivity by using Gd complexes endowed with a shorter exchange lifetime thus removing the observed quenching effect of τ_M on the relaxivity. It could also be improved in terms of stability by using a multifunctionalized Gd^{III} chelate of higher affinity and through the modification of the nanoparticle surface with hydrophilic polymers, such as poly(ethylene glycol), to control the in vivo fate. All these studies are in progress and will be reported in due course.

Experimental Section

Unless stated otherwise, the chemicals were obtained from commercial sources and used without any additional purification. β-Cyclodextrin polymers (pβCD) were prepared by cross-linking β-cyclodextrin (βCD) with epichlorohydrin (EP), under strongly alkaline conditions.[80] The βCD content, as determined by ^{1}H NMR spectroscopy, was 70% w/w. The molar masses of the polymers obtained were between 10^6 and 2.6×10^6 $g\,mol^{-1}$, as determined by gel filtration chromatography.[80] To synthesize dextran bearing lauryl side chains (MD), lauryl chloride was linked to the dextran polymer and subsequently purified by precipitation and dialysis. The substitution yield of MD was determined according to the ^{1}H NMR spectra and was found to be 4.3%, according to the amount of lauryl chloride introduced in the reaction mixture.[46] Reactions were monitored by thin-layer chromatography (TLC) performed on precoated silica gel (F254, Merck) or RP-18 (F254, Merck) plates. Plates were visualized under UV light (254 nm), and using Dragendorff reagent. Compounds containing unmetalated cyclen could be easily detected using a platinum stain.[81] Silica gel 60 (particle size 40–63 μM) was used for flash column chromatography. Ion exchange chromatography was performed with AG1-X4 ion exchange resin (100–200 Mesh, Bio-Rad) and gel filtration chromatography was performed using Sephadex G10 resin (Pharmacia). ^{1}H and ^{13}C NMR spectra were recorded at 300, 500 and 600 MHz (Bruker spectrometers), at 298 K (or 373 K for compound **3**), in deuterated solvents and calibrated against the solvent residual peak. Chemical shifts are given in ppm relative to TMS as an external standard. Mass spectra (MS) and high-resolution mass spectra (HRMS) were recorded using electro spray ionization (ESI) conditions in a positive-ion or a negative-ion mode (MALDI-TOF mass spectrometer Voyager-DE STR, Applied Biosystems).

Synthesis of Gd complex 5

*N-(1-Adamantyl)-2-bromoacetamide (**1**)*: An aqueous solution of 1 N NaOH (17.0 mL, 17.0 mmol) was slowly added to a cooled solution of 1-adamantylamine hydrochloride (3.0 g, 16.0 mmol) in water (20 mL). The resulting suspension was extracted with CH_2Cl_2 (5×25 mL). The combined organic phases were dried (Na_2SO_4), filtered, and evaporated under reduced pressure to give 1-adamantanamine. A solution of bromo acetyl bromide (2.90 g, 14.4 mmol) in CH_2Cl_2 (10 mL) was then added dropwise over a period of 30 min to a cooled suspension of Na_2CO_3 (1.90 g, 17.6 mmol) and the previously obtained 1-adamantanamine in CH_2Cl_2 (40 mL). After completion of the addition the mixture was stirred at room temperature for one more hour and water (50 mL) was added to the solution. The organic phase was successively washed with water, with 1 N aqueous HCl and with brine. After drying (Na_2SO_4) and evaporation of the solvent under reduced pressure a white solid was obtained that was crystallized in toluene to give **1** as colorless crystals (1.0 g, 73%). M.p. 127–128 °C (lit.[58] 124–126 °C from benzene); TLC (Silica, CH_2Cl_2): $R_f=0.53$; ^{1}H NMR (300 MHz , $CDCl_3$): $\delta=1.66$–1.71 (m, 6H; 3CH_2 Ad), 1.99–2.03 (m, 6H; 3CH_2 Ad), 2.06–2.13 (m, 3H; 3CH Ad), 3.77 (s, 2H; CH_2Br), 6.11 ppm (sl, 1H; NH); ^{13}C NMR (300 MHz , $CDCl_3$): $\delta=$ 29.26(3) (CH Ad), 29.83 (CH_2Br), 36.12(3) (CH_2 Ad), 41.06(3) (CH_2 Ad), 52.43 (CAdNH), 164.07 ppm (C=O); MS(ESI): *m/z*: 273 $[M+H]^+$, 295 $[M+Na]^+$, 311 $[M+K]^+$.

*Triethyl 2,2′,2″-{10-[2-(1-adamantylamino)-2-oxoethyl]-1,4,7,10-tetraazacyclodo-decane-1,4,7-triyl}triacetate (**3**)*: Bromoacetamide **1** (0.95 g, 3.49 mmol) was added to a stirred suspension of DO3A triester **2** (1.50 g, 3.49 mmol) and K_2CO_3 (1.73 g, 10,5 mmol) in acetonitrile (10 mL). After 4 h at room temperature, the suspension was filtered and the precipitate washed with acetonitrile. The solvent was evaporated under reduced pressure and the yellow residue was purified by flash chromatography on deactivated silica gel (deactivation with CH_2Cl_2/33% Me_3N-EtOH, 9:1; eluent: CH_2Cl_2/EtOH 9:1) to afford compound **2** (2.10 g, 97%) as a white powder. TLC (RP18, CH_3CN/H_2O/TFA = 1:1:0.1): $R_f=0.39$; ^{1}H NMR (500 MHz, $[D_6]$DMSO, 373 K): $\delta=1.20$–1.28 (m, 9H; 3CH_3CH_2), 1.60–1.72 (m, 6H; 3CH_2Ad), 1.94–2.01 (m, 6H; 3CH_2Ad), 2.01–2.09 (m, 3H; CHAd), 2.54–3.28 (m, 16H; CH_2 Cyclen), 3.28–3.53 (m, 6H; NCH_2CO), 4.10–4.23 (m, 6H; 3CH_3CH_2-O), 7.33 ppm (s, 1H; NH); ^{13}C NMR (150 MHz, $[D_6]$DMSO): $\delta=14.39$ (CH_3CH_2), 29.30 (CHAd), 36.41 (CH_2NAd), 41.25 (CH*C*H_2Ad), 50.56–51.23 (CH_2 cyclen), 51.65 (*C*AdNHCO), 55.34 (N*C*H_2COO), 55.42 (NCH_2COO), 57.37 (NCH_2CONH, CAd, CH_2 cyclen and CH_2CO), 60.92 (CH_2CH_3), 171.35 (CONH), 172.80 ($COOCH_2$), 173.47 ppm ($COOCH_2$); HPLC-MS (Column: Symmetry Shield 5 μm 4.6×150 mm; eluent A: H_2O, HCOOH 0.01% (v/v) B: CH_3CN, HCOOH 0.01% (v/v), flow: 1 mL/min, linear gradient from 90% A to 70% A in 15 min. Detection: LSD and Mass detection: Electro spray ionization (ESI) in positive mode $[M]^+=622$), $R_t=$ 13.13 min; MS (ESI$^+$): *m/z*: 622 $[M+H]^+$, 644 $[M+Na]^+$; HRMS calcd for $C_{32}H_{56}N_5O_7$: 622.4180; found: 622.4163.

*2,2′,2″-{10-[2-(1-Adamantylamino)-2-oxoethyl]-1,4,7,10-tetraazacyclododecane-1,4,7-triyl}triacetic acid (**4**)*: A suspension of the triethyl ester **3** (2.0 g, 3.22 mmol) in EtOH (4 mL) was stirred overnight at room temperature in the presence of AG1-X4 resin (32 mL of wet resin, 32.2 mequiv, 100–200 mesh, OH form). The mixture was loaded on a glass column fitted at the bottom with a glass frit (17 mm diameter), and washed with water. The product was eluted with a 0.1 M solution of ammonium hydrogenocarbonate. The fractions containing the product were collected and freeze-dried. The solid residue was dissolved in water and freeze-dried again. This operation was repeated three times in order to completely eliminate the ammonium salts and to afford compound **4** (1.1 g, 56%). White powder, m.p.: 197 °C; TLC (RP18 silica gel, CH_3CN/H_2O/TFA, 1:1:0.1): $R_f=0.70$; ^{1}H NMR (600 MHz, $[D_6]$DMSO): $\delta=1.58$–1.64 (m, 6H; CH_2Ad), 1.92–1.98 (m, 6H; CH_2Ad), 1.98–2.02 (m, 3H; CHAd), 2.68–3.22 (m, 16H; CH_2Cyclen), 3.29 (s, 2H; CH_2CONH), 3.48 (s, 2H; CH_2COO), 3.56 (s, 4H; CH_2COO), 7.28 ppm (s, 1H; NH); ^{13}C NMR (150 MHz, $[D_6]$DMSO): $\delta=29.28(3)$ (CHAd), 36.46(3) (*C*H_2CHAd), 41.25(3) (*C*H_2CNAd), 50.28, 50.31, 50.36, 51.24 (CH_2cyclen) 51.54 (*C*AdNHCO), 55.50 (*C*H_2CONH), 57.59(3) (*C*H_2COO), 168.49(CONH), 170.74(2) (COO), 171.62 ppm (COO); HPLC-MS (Column: Symmetry Shield 5 μm 4.6×150 mm; eluent A: H_2O, HCOOH 0.01% (v/v) B: CH_3CN, HCOOH 0.01% (v/v), flow: 1 mL min^{-1}, stepwise gradient from 90% A to 70% A in 15 min and from 70% A to 50% A in 15 min. Detection: LSD and Mass detection: Electro spray ionization (ESI) in negative mode $[M-H]^-=536$), $R_t=7.97$ min; ESI$^-$: 536 $[M-H]^+$; HRMS calcd for $C_{26}H_{42}N_5O_7$: 536.3084; found: 536.3173.

*Gadolinium complex of 2,2′,2″-[10-[2-(1-adamantylamino)-2-oxoethyl]-1,4,7,10-tetraazacyclododecane-1,4,7-triyl]triacetic acid (**5**)*: A solution of $GdCl_3 \cdot H_2O$ (0.054 g, 0.21 mmol) in water (2 mL) at pH 4.6 was slowly added to a solution of triacid **4** (0.10 g, 0.19 mmol) in water (2 mL). The pH of the solution was continuously adjusted to 6.5 by addition of 1 N NaOH. After completion of the addition, the pH was increased to 7.5 and the reaction was stirred for 60 h at room temperature. The pH was then increased to 9 in order to precipitate all the excess Gd^{III} as $Gd(OH)_3$. The solution was filtered (0.2 μm Millipore filter for syringe) and freeze-dried, to afford the compound **5** as a white solid (0.15 g). The Gd^{III} chelate was further purified from salts by gel filtration (Sephadex G10, 1.2×80 cm) eluting with water. The collected fractions were freeze-dried, to afford the compound **5** as a white solid with a purity of 98% determined by Evans' method[46] (0.11 g, 76%); Maldi MS: *m/z*: 693.22 $[M]^+$, 715.21 $[M+Na]^+$; HRMS calcd for $C_{26}H_{41}N_5O_7Gd$: 693.22695; found: 693.22416. HPLC-MS (Column: Sunfire 5 μm 4.6×150 mm; eluent A: Ammonium acetate 25 mM B:CH_3CN, linear gradient from 100% A to 70% A and 30% B in 30 min. Mass detection: Electro spray ionization (ESI) in positive mode $[M]^+ = 693$), $R_t = 13.59$ min.

Nanoparticles preparation and characterization:

General procedure for the preparation: Stock solutions of pβCD/**5** were first obtained by adding Gd complex **5** as a solid (0.5 to 6 mg mL^{-1} final concentration) to an aqueous solution of pβCD (2.5 or 5 mg mL^{-1}) and stirring overnight at RT. MD stock solutions were obtained by dissolution of MD in water at concentration of 2.5 or 5 mg mL^{-1} with stirring at RT overnight.

Nanoparticles containing **5** were then obtained by mixing at room temperature equal volumes (0.5–1 mL) of these two stock solutions. For the study of the effect of the component ratio on the size, stability, and **5** entrapment of the nanoparticles, three different preparations were used. They were obtained using the stock solutions S1 and S2 with the following concentrations of the three components:

Preparation A: S1) 5 mg mL^{-1} of pβCD and 1 mg mL^{-1} of **5**; S2) 5 mg mL^{-1} of MD.

Preparation B: S1) 2.5 mg mL^{-1} of pβCD and 1 mg mL^{-1} of **5**; S2) 2.5 mg mL^{-1} of MD.

Preparation C: S1) 2.5 mg mL^{-1} of pβCD and 0.5 mg mL^{-1} of **5**; S2) 2.5 mg mL^{-1} of MD.

For the evaluation of the maximum amount of **5** that can be entrapped, two other preparations were obtained using the same procedure. Stock solutions S1 and S2 with the following concentrations of the three components were used:

1) S1) 5 mg mL^{-1} of pβCD and 4 mg mL^{-1} of **5**; S2) 5 mg mL^{-1} of MD

2) S1) 5 mg mL^{-1} of pβCD and 6 mg mL^{-1} of **5**; S2) 5 mg mL^{-1} of MD.

Size measurements: The mean diameter and the size distribution of the nanoparticles were determined at different time intervals, after their formation, by quasi-elastic light scattering (QELS) by using a Coulter nanosizer (model N4 MD, Coultronic, France). According to need, samples were diluted with milliQ water in order to maintain the count per second between 5×10^4 and 1×10^6. Each measurement was repeated three times for two minutes at room temperature (20–25 °C) and at 37 °C, at an angle of 90°.

*Quantification of the **5** entrapped*: Nanoparticle suspensions were centrifuged (25,000 g, 45 min, ultracentrifuge Beckmann Coulter LE-80 K), using a 50.3 Ti rotor, in order to remove the non-entrapped **5**. The amount of **5** entrapped in the nanoparticles was determined as the difference between the total amount of Gd^{III} chelate added and the amount of Gd^{III} chelate detected in the supernatant. The percentage of entrapment was calculated as the ratio between amount of entrapped Gd^{III} chelate and the total amount of Gd^{III} chelate added. The amount of **5** in the supernatant was determined by Evans' method.[46] For this *tert*-butanol (25 μL) was added as standard to a sample of supernatant (500 μL). ^{1}H NMR spectra were acquired (500 MHz, 298 K) in presence of an inner cell containing external standard consisting of D_2O (100 μL) and *tert*-butanol (25 μL). By measuring the difference of chemical shift, $\Delta(\delta)$ in ppm, between the signals of *tert*-butanol from the two solutions, it was possible to calculate the exact amount of paramagnetic agent present in solution, by Equation (7), in which *c* is the concentration of the Gd^{III} chelate, $s = 1/3$ (for cryomagnet), μ_{eff} is the magnetic moment of the lanthanide metal (7.94 for Gd^{III}).

$$\Delta(\delta) = (4000\pi cs/T)\,(\mu_{eff}/2.84)^2 \qquad (7)$$

Stability of the entrapment: The stability of the entrapment was evaluated by quantifying the **5** entrapped as described above, at different time intervals after the preparation, over a period of 36 h.

Water proton relaxivity measurements: The longitudinal water proton relaxation rate was measured by using a Stelar Spinmaster (Stelar, Mede, Pavia, Italy) spectrometer operating at 20 MHz, by mean of the standard inversion–recovery technique. The temperature was controlled with a Stelar VTC-91 air-flow heater equipped with a copper constantan thermocouple (uncertainty 0.1 °C). The proton $1/T_1$ NMRD profiles were measured over a continuum of magnetic field strength from 0.00024 to 0.47 T (corresponding to 0.01–20 MHz proton Larmor Frequency) on a Stelar field-cycling relaxometer. The relaxometer works under complete computer control with an absolute uncertainnty in $1/T_1$ of ±1%. Data points from 0.47 T (20 MHz) to 1.7 T (70 MHz) were collected on a Stelar Spinmaster spectrometer working at variable field. The concentration of the **5** solution, for the relaxometric characterization, was determined by mineralizing a given quantity of sample solution by the addition of HCl 37% at 120 °C overnight: from the measurement of the observed relaxation rate (R_{1obs}) of the acidic solution and knowing the relaxivity (r_{1p}) of Gd^{III} aquation in acidic conditions (13.5 mM^{-1}s^{-1}), it was possible to calculate the exact Gd^{III} concentration (this method was calibrated using standard ICP solutions, and the accuracy was determined to be 1%).

Variable-temperature ^{17}O measurements: For ^{17}O measurements, aqueous solution containing 2.6% ^{17}O isotope (Yeda, Israel) was used. Variable-temperature ^{17}O NMR measurements were recorded at 600 MHz on a Bruker spectrometer, equipped with a 5 mm probe, by using a D_2O external lock. Experimental settings were as follows: spectral width of 9000 Hz, 90° pulse for 14 μs, acquisition time 10 ms, 1024 scans and without sample spinning. The observed transverse relaxation rates $R^O_{2p\,obs}$ were calculated from the signal width at half-height ($\Delta\nu 1/2$): $R^O_{2p\,obs} = \pi\,\Delta\nu 1/2$.

The simultaneous least-squares fittings were performed with the program Origin 7.0 for Windows systems.

Acknowledgements

We thank M.-T. Adeline, F. Pelissier, and N. Loussaief for their help with the HPLC analysis, and J.-F. Gallard and O. Rakotonandrasana for performing NMR analysis. We thank R. Dodd for critical reading of the manuscript. Financial support from the Institute ICSN to E. Battistini and from the European network of excellence "EMIL" for laboratory exchanges is gratefully acknowledged.

[1] É. Tóth, L. Helm, A. E. Merbach, *Top. Curr. Chem.* **2002**, *221*, 61–101.

[2] É. Tóth, L. Helm, A. E. Merbach in *The Chemistry of Contrast Agents in Medicinal Magnetic Resonance Imaging* (Eds.: A. E. Merbach, É. Tóth), Wiley, Chischester, **2001**, pp. 45–119.

[3] P. Caravan, J. J. Ellison, T. J. McMurry, R. B. Lauffer, *Chem. Rev.* **1999**, *99*, 2293–2352.

[4] R. B. Lauffer, *Chem. Rev.* **1987**, *87*, 901–927.

[5] D. E. Sosnovik, R. Weissleder, *Curr. Opin. Biotechnol.* **2007**, *18*, 4–10.

[6] Z. Zhang, M. T. Greenfield, M. Spiller, T. J. McMurry, R. B. Lauffer, P. Caravan, *Angew. Chem.* **2005**, *117*, 6924–6927; *Angew. Chem. Int. Ed.* **2005**, *44*, 6766–6769.

[7] P. M. Winter, S. D. Caruthers, S. A. Wickline, G. M. Lanza, *Curr. Cardiol. Rev.* **2006**, *8*, 65–69.

[8] S. D. Caruthers, P. M. Winter, S. A. Wickline, G. M. Lanza, *Methods Mol. Med.* **2006**, *124*, 387–400.
[9] A. Jasanoff, *Trends Neurosci.* **2005**, *28*, 120–126.
[10] D. Artemov, Z. M. Bhujwalla, J. W. M. Bulte, *Curr. Pharm. Biotechnol.* **2004**, *5*, 485–494.
[11] P. Caravan, *Chem. Soc. Rev.* **2006**, *35*, 512–523.
[12] S. Langereis, A. Dirksen, T. M. Hackeng, M. H. P. van Genderen, E. W. Meijer, *New J. Chem.* **2007**, *31*, 1152–1160.
[13] Z.-R. Lu, Y. Wang, F. Ye, A. Vaidya, E.-K. Jeong, *Nanotechnology* **2007**, 201–212.
[14] C. B. Sirlin, D. R. Vera, J. A. Corbeil, M. B. Caballero, R. B. Buxton, R. F. Mattrey, *Acad. Radiol.* **2004**, *11*, 1361–1369.
[15] J. P. Andre, C. F. Geraldes, J. A. Martins, A. E. Merbach, M. I. Prata, A. C. Santos, J. J. de Lima, É. Tóth, *Chem. Eur. J.* **2004**, *10*, 5804–5816.
[16] P. Lebduskova, J. Kotek, P. Hermann, L. Vander Elst, R. N. Muller, I. Lukes, J. A. Peters, *Bioconjugate Chem.* **2004**, *15*, 881–889.
[17] V. P. Torchilin, *Curr. Pharm. Biotechnol.* **2000**, *1*, 183–215.
[18] F. Ye, T. Ke, E.-K. Jeong, X. Wang, Y. Sun, M. Johnson, Z.-R. Lu, *Mol. Pharm.* **2006**, *3*, 507–515.
[19] S. Aime, M. Botta, M. Fasano and E. Terreno in *Protein-Bound Metal Chelates in Chemistry of Contrast Agents in Medical Magnetic Resonance Imaging* (Eds.: A. E. Merbach, É. Tóth), Wiley, Chichester, **2001**, pp. 193–241.
[20] J. B. Livramento, A. Sour, A. Borel, A. E. Merbach, E. Toth, *Chem. Eur. J.* **2006**, *12*, 989–1003.
[21] C.-Y. Shu, E.-Y. Zhang, J.-F. Xiang, C.-F. Zhu, C.-R. Wang, X.-L. Pei, H.-B. Han, *J. Phys. Chem. B* **2006**, *110*, 15597–15601.
[22] S. R. Bull, M. O. Guler, R. E. Bras, P. N. Venkatasubramanian, S. I. Stupp, T. J. Meade, *Bioconjugate Chem.* **2005**, *16*, 1343–1348.
[23] J. B. Livramento, E. Toth, A. Sour, A. Borel, A. E. Merbach, R. Ruloff, *Angew. Chem.* **2005**, *117*, 1504–1508; *Angew. Chem. Int. Ed.* **2005**, *44*, 1480–1484.
[24] A. Accardo, D. Tesauro, P. Roscigno, E. Gianolio, L. Paduano, G. D'Errico, C. Pedone, G. Morelli, *J. Am. Chem. Soc.* **2004**, *126*, 3097–3107.
[25] N. Fatin-Rouge, É. Tóth, R. Meuli, J.-C. G. Bünzli, *J. Alloys Compd.* **2004**, *374*, 298–302.
[26] K. Kimpe, T. N. Parac-Vogt, S. Laurent, C. Piérart, L. Vander Elst, R. N. Muller, K. Binnemans, *Eur. J. Inorg. Chem.* **2003**, *3021*–3027.
[27] V. P. Torchilin, *Adv. Drug Delivery Rev.* **2002**, *54*, 235–252.
[28] J. P. André, É. Tóth, H. Fischer, A. Seelig, H. R. Mäcke, A. E. Merbach, *Chem. Eur. J.* **1999**, *5*, 2977–2983.
[29] V. Comblin, D. , M. Gilsoul, V. Hermann, V. Humblet, J. Mesbahi, M. C. Sauvage, *Coord. Chem. Rev.* **1999**, *451*–470.
[30] S. G. Crich, C. Cabella, A. Barge, S. Belfiore, C. Ghirelli, L. Lattuada, S. Lanzardo, A. Mortillaro, L. Tei, M. Visigalli, G. Forni, S. Aime, *J. Med. Chem.* **2006**, *49*, 4926–4936.
[31] S. Geninatti Crich, A. Barge, E. Battistini, C. Cabella, S. Coluccia, D. Longo, V. Mainero, G. Tarone, S. Aime, *J. Biol. Inorg. Chem.* **2005**, *10*, 78–86.
[32] S. Aime, I. M. Botta, F. Fedeli, E. Gianolio, E. Terreno, P. Anelli, *Chem. Eur. J.* **2001**, *7*, 5261–5269.
[33] W. J. Mulder, G. J. Strijkers, G. A. van Tilborg, A. W. Griffioen, K. Nicolay, *NMR Biomed.* **2006**, *19*, 142–164.
[34] S. Erdogan, A. Roby, R. Sawant, J. Hurley, V. Torchilin, *J. Liposome Res.* **2006**, *16*, 45–55.
[35] G. M. Lanza, P. M. Winter, S. D. Caruthers, M. S. Hughes, T. Cyrus, J. N. Marsh, A. M. Neubauer, K. C. Partlow and S. A. Wickline, *Nanomedicine***2006**, *1*, 321–329.
[36] S. W. Zielhuis, J.-H. Seppenwoolde, V. A. P. Mateus, C. J. G. Bakker, G. C. Krijger, G. Storm, B. A. Zonnenberg, A. D. van het Schip, G. A. Koning, J. F. W. Nijsen, *Cancer Biother. Radiopharm.* **2006**, *21*, 520–527.
[37] D. Zhu, R. D. White, P. A. Hardy, N. Weerapreeyakul, K. Sutthanut, M. Jay, *J. Nanosci. Nanotechnol.* **2006**, *6*, 996–1003.
[38] L. E. van Vlerken, M. M. Amiji, *Expert Opin. Drug Delivery* **2006**, *3*, 205–216.
[39] D. Mislovicova, G. Kogan, N. M. Gosselet, B. Sebille, L. Soltes, *Chem. Biodiversity* **2007**, *4*, 52–57.
[40] A. Harada, *JJ. Polym. Sci. Part A* **2006**, *44*, 5113–5119.
[41] S. Aime, E. Gianolio, F. Uggeri, S. Tagliapietra, A. Barge, G. Cravotto, *J. Inorg. Biochem.* **2006**, *100*, 931–938.
[42] S. Aime, M. Botta, E. Gianolio, E. Terreno, *Angew. Chem.* **2000**, *112*, 763–766; *Angew. Chem. Int. Ed.* **2000**, *39*, 747–750.
[43] S. Aime, E. Gianolio, E. Terreno, G. B. Giovenzana, R. Pagliarin, M. Sisti, G. Palmisano, M. Botta, M. P. Lowe, D. Parker, *J. Biol. Inorg. Chem.* **2000**, *5*, 488–497.
[44] S. Aime, M. Botta, L. Frullano, S. G. Crich, G. B. Giovenzana, R. Pagliarin, G. Palmisano, M. Sisti, *Chem. Eur. J.* **1999**, *5*, 1253–1260.
[45] S. Aime, M. Botta, M. Fasano, S. Geninatti Crich, E. Terreno, *Coord. Chem. Rev.* **1999**, *185*–186, 321–333.
[46] R. Gref, C. Amiel, K. Molinard, S. Daoud-Mahammed, B. Sebille, B. Gillet, J. C. Beloeil, C. Ringard, V. Rosilio, J. Poupaert, P. Couvreur, *J. Controlled Release* **2006**, *111*, 316–324.
[47] R.Gref, P. Couvreur, unpublished result.
[48] M. V. Rekharsky, Y. Inoue, *Chem. Rev.* **1998**, *98*, 1875–1917.
[49] K. A. Connors, *Chem. Rev.* **1997**, *97*, 1325–1357.
[50] J. Carrazana, A. Jover, F. Meijide, V. H. Soto, J. Vàzquez Tato, *J. Phys. Chem. B* **2005**, *109*, 9719–9726.
[51] F. P. Charbonnier, *Eur. J. Org. Chem.* **2004**, *3650*–3656.
[52] V. H. Tellini, A. Jover, L. Galantini, F. Meijide, J. V. Tato, *Acta Crystallogr. Sect. B* **2004**, *60*, 204–210.
[53] M. Czugler, E. Eckle, J. J. Stezowski, *J. Chem. Soc. Chem. Commun.* **1981**, *24*, 1291–1292.
[54] V. Burckbuchler, V. Boutant, V. Wintgens, C. Amiel, *Biomacromolecules* **2006**, *7*, 2890–2900.
[55] S. Aime, M. Botta, M. Fasano, S. Paoletti, P. L. Anelli, F. Uggeri, M. Virtuani, *Inorg. Chem.* **1994**, *33*, 4707–4711.
[56] G. Gonzalez, D. H. Powell, V. Tissières, A. E. Merbach, *J. Phys. Chem.* **1994**, *98*, 53–59.
[57] Y.-M. Wang, S.-T. Lin, Y.-J. Wang, R.-S. Sheu, *Polyhedron* **1998**, *17*, 2021–2028.
[58] J. Pospisil, M. Travnicek, M. Potacek, *ARKIVOC* **2001**, *146*–162.
[59] S. Aime, C. S. Geninatti, E. Gianolio, E. Terreno, A. Beltrami, F. Uggeri, *Eur. J. Inorg. Chem.* **1998**, *1283*–1289.
[60] S. Aime, M. Botta, G. Ermondi, E. Terreno, P. L. Anelli, F. Fedeli, F. Uggeri, *Inorg. Chem.* **1996**, *35*, 2726–2736.
[61] S. Aime, M. , M. Botta, M. Panero, M. Grandi, F. Uggeri, *Magn. Reson. Chem.* **1991**, *29*, 923–927.
[62] S. J. Ratnakar, A. Vedhamonickom, *Eur. J. Inorg. Chem.* **2005**, *3918*–3927.
[63] S. Aime, S. G. Crich, E. Gianolio, E. Terreno, A. Beltrami, F. Uggeri, *Eur. J. Inorg. Chem.* **1998**, *1283*–1289.
[64] S. Aime, F. Benetollo, G. Bombieri, S. Colla, M. Fasano, S. Paoletti, *Inorg. Chim. Acta* **1997**, *245*, 63–70.
[65] E. C. Wiener, M. W. Brechbiel, H. Brothers, R. L. Magin, O. A. Gansow, D. A. Tomalia, P. C. Lauterbur, *Magn. Reson. Med.* **1994**, *31*, 1–8.
[66] D. M. Corsi, C. Platas-Iglesias, H. van Bekkum, *Magn. Reson. Chem.* **2001**, *39*, 723–726.
[67] R. Gref, Y. Minamitake, M. T. Peracchia, V. Trubetskoy, V. Torchilin, R. Langer, *Science* **1994**, *263*, 1600–1603.
[68] A. M. Morawski, P. M. Winter, K. C. Crowder, S. D. Caruthers, R. W. Fuhrhop, M. J. Scott, J. D. Robertson, D. R. Abendschein, G. M. Lanza, S. A. Wickline, *Magn. Reson. Med.* **2004**, *51*, 480–486.
[69] G. J. Strijkers, W. J. Mulder, R. B. van Heeswijk, P. M. Frederik, P. Bomans, P. C. Magusin, K. Nicolay, *Magn. Reson. Mater. Phys. Biol. Med.* **2005**, *18*, 186–192.
[70] U. Frey, A. E. Merbach and D. H. Powell in *Dynamics of Solutions and Fluid Mixtures by NMR* (Ed.: J.-J. Delpuech), Wiley, Chichester (UK), **1995**, pp. 263–307.
[71] T. J. Swift, R. E. Connick, *J. Chem. Phys.* **1962**, *37*, 307–320.
[72] D. H. Powell, O. M. N. Dhubhghaill, D. Pubanz, L. Helm, Y. S. Lebedev, W. Schlaepfer, A. E. Merbach, *J. Am. Chem. Soc.* **1996**, *118*, 9333–9346.

[73] Jaszberenyi, A. Sour, E. Toth, M. Benmelouka, A. E. Merbach, *Dalton Trans.* **2005**, *2713*–2719.
[74] M.-H. Ou, Y.-M. Chen, Y.-H. Chang, W.-K. Lu, G.-C. Liu, Y.-M. Wang, *Dalton Trans.* **2007**, *2749*–2759.
[75] N. Blombergen, *J. Chem. Phys.* **1957**, *27*, 572–573.
[76] I. Solomon, *Phys. Rev.* **1955**, *99*, 559–565.
[77] J. H. Freed, *J. Chem. Phys.* **1978**, *68*, 4034–4037.
[78] S. M. Cohen, J. Xu, E. Radkov, K. N. Raymond, M. Botta, A. Barge, S. Aime, *Inorg. Chem.* **2000**, *39*, 5747–5756.
[79] M. Botta, *Eur. J. Inorg. Chem.* **2000**, *399*–407.
[80] E. Renard, A. Deratani, G. Volet, B. Sebille, *Eur. Polym. J.* **1997**, *33*, 49–57.
[81] J. A. Duimstra, F. J. Femia, T. J. Meade, *J. Am. Chem. Soc.* **2005**, *127*, 12847–12855.

Received: October 8, 2007
Published online: April 2, 2008

